

# Distributions of stresses and geometry of the Wadati-Benioff zone under Chiapas, Mexico

Cecilio J. Rebollar<sup>1</sup>, Victor H. Espíndola<sup>1</sup>, Antonio Uribe<sup>2</sup>, Antonio Mendoza<sup>1</sup> and Arturo Pérez-Vertti<sup>1</sup>

<sup>1</sup> CICESE, Earth Science Division, Baja California, Mexico.

<sup>2</sup> CFE, Gerencia de Estudios de Ingeniería Civil, Departamento de Sismotectónica, México D. F.

Received: June 15, 1998; accepted: November 30, 1998.

## RESUMEN

La sismicidad registrada desde junio de 1994 a mayo de 1995, en una red portátil de estaciones sismológicas analógicas y digitales, definieron la geometría de la zona Wadati-Benioff bajo Chiapas, así como la distribución de los esfuerzos principales en la placa subducida. La sismicidad localizada en el antearco no fue bien localizada. Un módulo de Poisson de 0.24 fue calculado para la corteza de Chiapas. 321 sismos fueron localizados en el rango de magnitudes entre 3.3 y 5.6. Los hipocentros definieron la zona Wadati-Benioff de  $39 \pm 4$  km de grueso buzando  $40^\circ \pm 3^\circ$  hacia N45°E. La profundidad de los sismos varió entre 10 a 300 km. La placa de Cocos buza aproximadamente  $25^\circ$  en Oaxaca,  $30^\circ$  bajo el Golfo de Tehuantepec y  $40^\circ$  hacia el sudeste. Un fuerte cambio en el buzamiento de la placa de Cocos ocurre en la intersección de la cordillera de Tehuantepec y la Trinchera de Centro América. La sismicidad en esta zona es difusa hasta profundidades de 200 km. Nuestros datos sugieren un incremento gradual del buzamiento de la placa de Cocos de Oaxaca a Chiapas. Los mecanismos focales de eventos con profundidades menores de 50 km indican que la placa subducida está bajo tensión, mientras que a profundidades entre 50 y 200 km la placa experimenta un régimen mixto de esfuerzos. A profundidades entre 200 y 300 km la litosfera subducida está bajo un régimen comprensivo en la dirección del buzamiento.

**PALABRAS CLAVE:** Sismicidad, zona de Wadati-Benioff, mecanismos focales, distribución de esfuerzos.

## ABSTRACT

Seismicity recorded from June 1994 to May 1995 on a portable network of analog and digital seismic stations defines the geometry of the Wadati-Benioff zone under Chiapas and the distributions of the principal stresses along the subducted slab. Seismicity at the outer-rise region is not well located. A Poisson's ratio of 0.24 was calculated for the crust of Chiapas. We located 321 earthquakes in the magnitude range from 3.3 to 5.6. Hypocenters define a Wadati-Benioff zone  $39 \pm 4$  km thick dipping  $40^\circ \pm 3^\circ$  to N45° E. Earthquake depths range from 10 km to 300 km. The Cocos plate dips nearly  $25^\circ$  in Oaxaca,  $30^\circ$  to  $35^\circ$  under the Gulf of Tehuantepec and  $40^\circ$  to the Southeast. A major change in dip occurs at the intersection of the Tehuantepec Ridge with the Middle America Trench. Seismicity in this zone is diffuse to depths of 200 km. Our data suggests a gradual increase of the dip of the Cocos plate from Oaxaca to Chiapas. Focal mechanisms of events with depths less than 50 km indicate that the subducted crust is under tension in this region, while at depths between 50 and 200 km there is a mixed pattern of stress distribution. At depths from 200 to 300 km the subducted lithosphere is under down-dip compression.

**KEY WORDS:** Seismicity, Wadati-Benioff zone, focal mechanisms, stress distribution.

## INTRODUCTION

A rapid convergence rate of the Cocos plate beneath the North America plate in Chiapas, and moderate interplate coupling (Thatcher, 1990) produce a high level of seismicity of the forearc and the subducted lithosphere. The state of Chiapas, in southeastern Mexico, is located near the triple junction of the North America, Cocos, and Caribbean plates. However, the location of the triple junction is not well defined. It comprises a broad zone of deformation in Chiapas and western Guatemala (Guzmán-Speziale, 1989). The Polochic-Motagua strike slip fault is located in Guatemala, at the boundary of the North America and Caribbean plates (Figure 1). In central Chiapas, there is a complex system of strike-slip, normal and thrust faults trending east west (see Figure 1). West of Chiapas, the most prominent tectonic feature is the Tehuantepec ridge, which acts as a transition zone in the morphology of the Middle America Trench (Singh and

Mortera, 1991; Pardo and Suárez, 1995). West of the Isthmus of Tehuantepec, the subducted lithosphere dips at an angle of  $25^\circ$  (Pardo and Suárez, 1995). At the Isthmus of Tehuantepec data analyzed by Ponce *et al.* (1992) suggest a dip of the W-B zone of  $38^\circ$ .

Havskov *et al.* (1982) located earthquakes at depths up to 200 km and estimated a dipping angle of the Wadati-Benioff (W-B) zone of  $45^\circ$ . These earthquakes were located with a seismic network located around Chicoasen dam (Figure 1). Burbach *et al.* (1984) found a W-B zone in Chiapas dipping  $26^\circ$  from the trench to a depth of 100 km, and from 100 to 200 km dipping at an angle of  $60^\circ$ . Bevis and Isacks (1984) estimated the maximum depth of the W-B zone at 200 km and an apparent thickness of 54 km of the slab in Chiapas and Central America. On the other hand, LeFevre and McNally (1985) found thrust events at shallow depths and normal events at depths of the order of 100 km. Ponce *et*

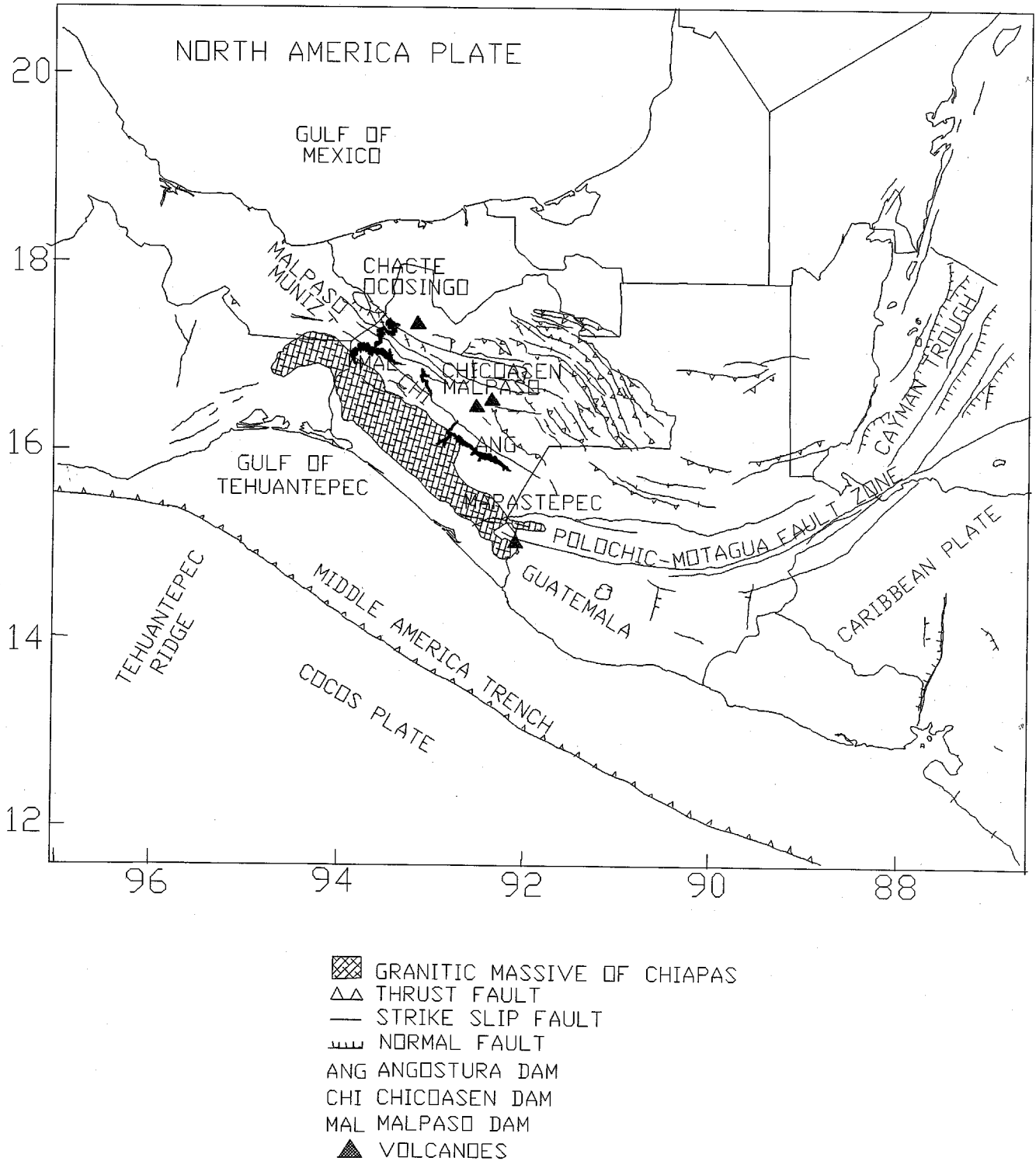


Fig. 1. Map showing tectonic features of the area of study. The Middle America Trench and the main structural features are shown. Strike slip faults, normal faults and thrust faults are also shown. Full triangles are volcanoes. Solid areas are reservoirs. Three lithospheric plates converge in Chiapas: Cocos, North America and Caribbean.

al. (1992) estimated a smooth increase of the dip of the subducted slab from east to west in the Isthmus of Tehuantepec region.

In this study, we use a portable array of short and broadband digital stations to supplement the short period analog seismic stations in Chiapas. The purpose of this paper is to

define the Wadati-Benioff (W-B) zone and the pattern of stress orientations in the subducted lithosphere.

### DATA ACQUISITION

We deployed a portable seismic network of analog and digital seismic stations in Chiapas in September of 1993. The array began recording in March of 1994. Five digital stations and three analog smoked paper recorders were deployed (see Figure 2 and Table 1). Reading errors of first arrival times were in the order of 0.1 seconds for analog stations,

and in the order of 0.01 seconds for digital stations. Geographical positions were calculated with a satellite positioning system. We used readings at Tapachula (TPX), San Cristobal (SCX) and Oaxaca (OXX) from the National Seismological Service of Mexico.

### SEISMICITY OF CHIAPAS

The Tehuantepec ridge roughly separates two distinct regions of seismic activity. West of the ridge the seismogenic zone extends down to a depth of 30 km, and the characteris-

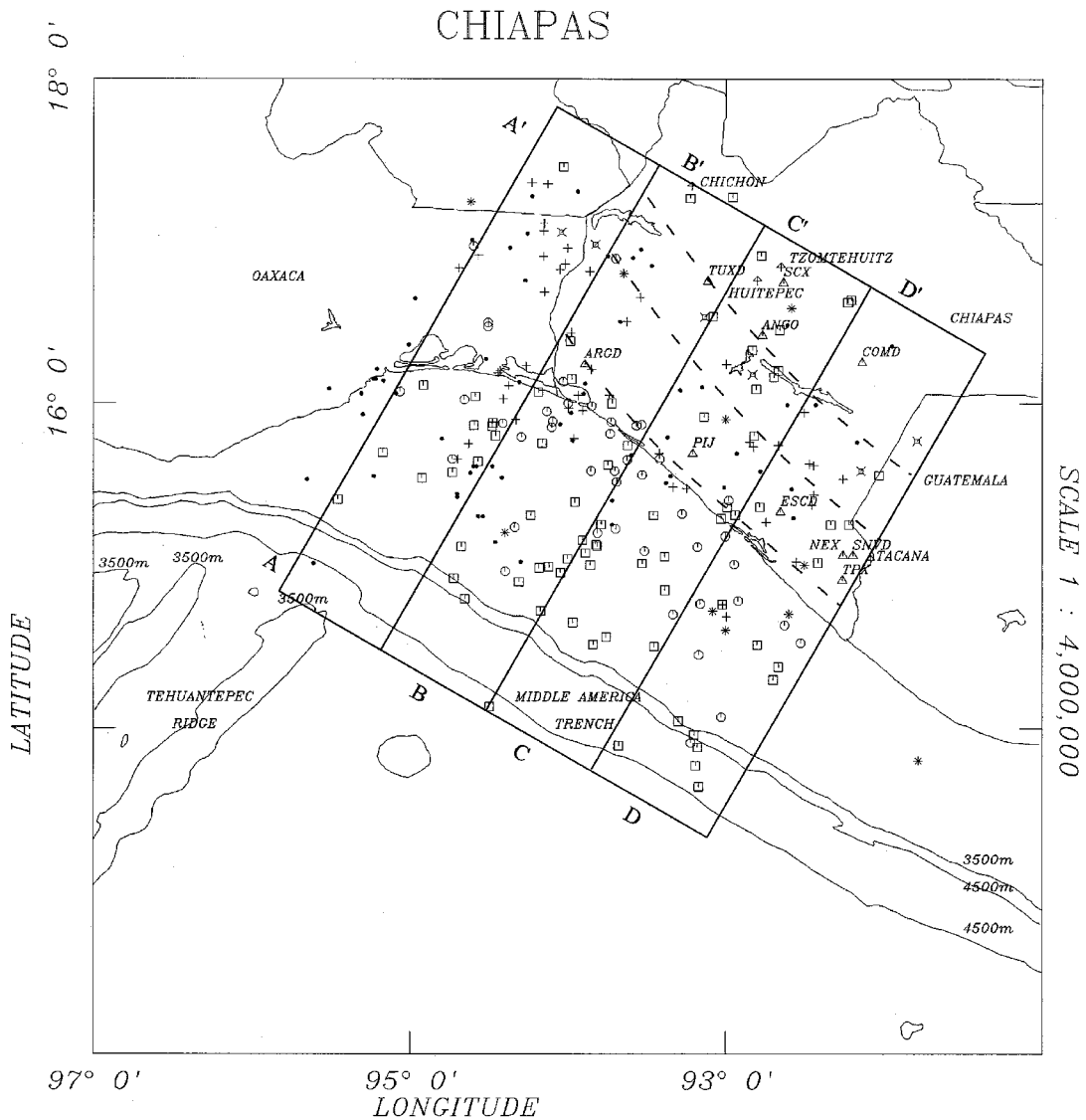


Fig. 2. Seismicity for one year of data acquisition. Open squares are events with hypocenters of depths less than 50 km. Circles are hypocenters with depths between 50 to 100 km, plus signs are those between 100 to 200 km, crosses with a dot are those between 200 to 300 km and stars are large events that occurred in this century. Solid dots are events with magnitudes greater than 5 reported by PDE from 1978 to 1995 and by Burbach *et al.* (1984). Vertical arrows are volcanoes and open triangles are seismic stations. Cross sections A-A', B-B', C-C' and D-D' are oriented in the direction of relative convergence of the Cocos plate. Isodepth contours of 100, 200, and 300 kilometers were projected from our data.

**Table 1**

Locations of seismic stations.

| STATION                 | LATITUDE (°N) | LONGITUDE (°W) | ELEVATION<br>meters | SITE<br>CHARACTERISTICS |
|-------------------------|---------------|----------------|---------------------|-------------------------|
| Angostura (ANGO)        | 16° 04.89 '   | 92° 46.04 '    | 500                 | Sedimentary Rock        |
| Arriaga (ARGD)          | 16° 44.28 '   | 93° 53.54 '    | 50                  | Granite                 |
| Comitán (COMD)          | 16° 15.00 '   | 92° 08.18 '    | 1500                | Sedimentary Rock        |
| Escuintla (ESCD)        | 15° 19.59 '   | 92° 37 08 '    | 100                 | Granite                 |
| Nexapa (NEX)            | 15° 03.51 '   | 92° 15.42 '    | 500                 | Sediment                |
| Pijijiapan (PIJ)        | 15° 01.58 '   | 93° 12.31 '    | 15                  | Granite                 |
| San Vicente (SNVD)      | 15° 03.42 '   | 92° 11.68 '    | 500                 | Andesite                |
| Tuxtla Gutiérrez (TUXD) | 16° 44.72 '   | 93° 06.78 '    | 500                 | Sedimentary Rock        |

tic earthquakes are in the magnitude range of 7 to 8.2. The Wadati-Benioff zone dips at an average angle of 25°. Hypocenters are not deeper than 100 km and large earthquakes have an interval of recurrence of about 30 years (Singh and Mortera, 1991; Pacheco *et al.*, 1993; Ruff and Miller, 1994; Pardo and Suárez, 1995). To the east of the ridge, the Wadati-Benioff zone dips at an angle of 40°, and characteristic earthquakes are in the magnitude range of 7 to 7.8. The seismogenic zone is not well defined; hypocenters are reportedly of the order of 300 km, and the intervals of recurrence are about 33 years (McNally and Minster, 1991; Singh *et al.*, 1981; Astiz and Kanamori, 1984; Pacheco and Sykes, 1992; Pacheco *et al.*, 1993).

Tehuantepec ridge is a possible seismic gap; no earthquake of magnitude greater than 7 occurred in this area at least in the last 190 years (Singh *et al.*, 1981; McCann *et al.*, 1979).

Hanus and Vanek (1978) found that the focal mechanisms of shallow events at the outer rise show normal faulting, and the events at the contact of the subducting and overriding plate show thrust faulting with one nodal plane parallel to the trench. Dean and Drake (1978) also found normal faulting in the outer rise region and thrust events in the Wadati-Benioff zone. Focal mechanisms of intermediate

events indicate that the subducted lithosphere is under extensional stress. Astiz *et al.* (1988) also found that shallow events have T axes along the down-dip direction.

### CRUSTAL VELOCITY STRUCTURE

Castro (1980) obtained an estimate of average crustal thickness in Chiapas. We used the Minimum Apparent Velocity (MAV) method for all seismic events recorded in Chiapas (Matumoto *et al.*, 1977; Suárez *et al.*, 1992; Ligorria and Ponce, 1993 and Ligorria and Molina, 1997). We chose azimuths less than 20° between pairs of stations and a ratio of epicentral distances less than  $\Delta_1/\Delta_2=0.66$ , where  $\Delta_1$  and  $\Delta_2$  are the epicentral distance to the stations. We located the events using S-P times from at least three seismic stations (see Lay and Wallace 1995, page 219). We plotted epicentral distance versus the apparent velocity defined as  $VA=\Delta d/\Delta t$  was  $\Delta d$  is the difference in epicentral distances and  $\Delta t$  is the difference in arrival times between the two stations. From Figure 3 we may distinguish three refracted wavefronts: a shallow velocity layer of 3.8 km/sec; a layer, with a velocity of 6.7 km/sec, related to the Conrad discontinuity, and the Moho discontinuity with a velocity of 8.2 km/sec. This method yields average velocities of the crust similar to those calculated by Castro (1980). Our velocity model is given in Table 2.

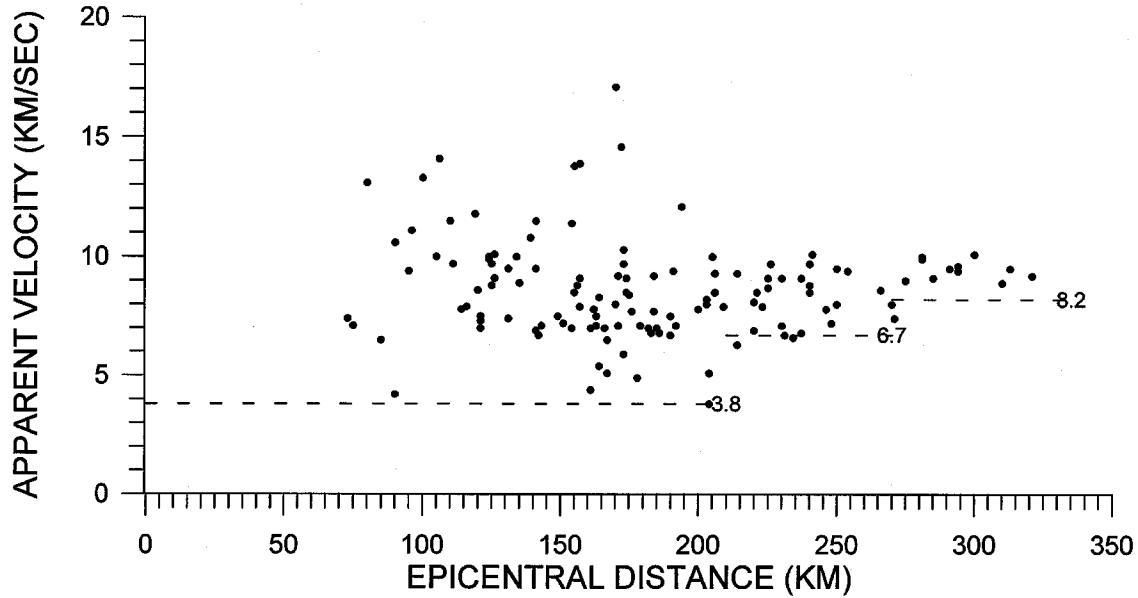


Fig. 3. Minimum apparent velocity plot. Each dot represents the apparent velocity VA as a function of epicentral distance. Three velocity layers with velocities of 3.8, 6.7 and 8.2 km/sec.

**Table 2**

Chiapas one-dimensional velocity structure.

| Depth (km) | P-wave velocity (km/s) | Density (gr/cm <sup>3</sup> ) |
|------------|------------------------|-------------------------------|
| 0          | 5                      | 2.7                           |
| 4          | 6.2                    | 2.9                           |
| 20         | 7                      | 3                             |
| 31         | 7.6                    | 3.1                           |
| 43         | 8.2                    | 3.4                           |

The Moho has a depth of 43 km in the strike-slip province (Malpaso-Muñiz and Chicoasen-Malpaso faults), as reported by Couch and Woodcock (1981). Under the Isthmus of Tehuantepec, Ligorria and Ponce (1993) reported a Moho depth of 38 km. In Guatemala, Ligorria and Molina (1997) estimated a maximum Moho depth of 46 km. Thus, within the uncertainties of the method, a slight increase of crustal thickness toward Central America is suggested. Offshore, the Moho depth is found at 15 km (Couch and Woodcock, 1981).

S-wave velocities can be estimated using Poisson's ratio. We used the Wadati diagram from S-P times ( $t_s - t_p$ ) versus origin time ( $T_o$ ) minus the P arrival time ( $T_o - p$ ). From the slope we obtained a ratio of  $V_p/V_s$  of 1.71 and a Poisson's ratio of 0.24 (Figure 4).

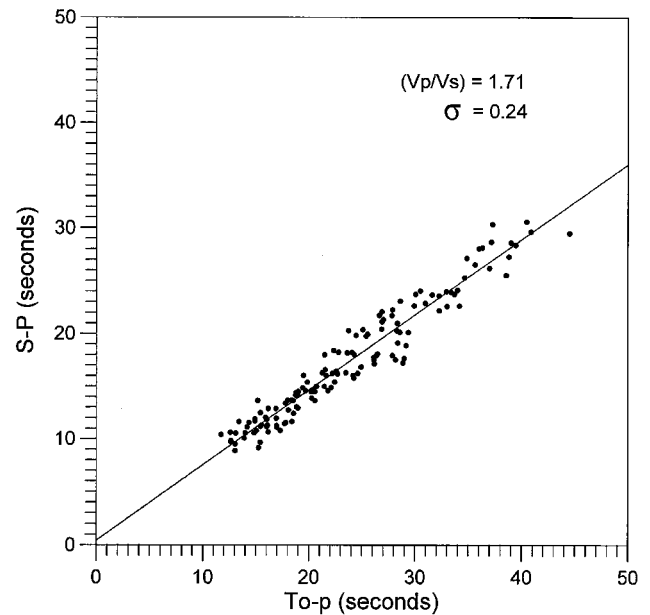


Fig. 4. Wadati diagram of selected data. We plotted S-P times versus origin time minus P time. From the slope we calculated a  $V_p/V_s$  value of 1.71 and a Poisson's ratio of 0.24.

### THE WADATI-BENIOFF ZONE

Earthquake locations were obtained with the program HYPO71 (Lee and Lahr, 1972) using the one-dimensional crustal model of Table 2. We located 321 events with magnitudes from 3.8 to 5.3 over a time span of twelve months. We selected events recorded at least in five stations with rms

(root mean square) errors of less than one second, except for events located offshore and in the Isthmus of Tehuantepec, where location errors are larger. Earthquake hypocenters range from 5 km depth to a maximum depth of 296 km.

Figure 2 shows the epicenters. Vertical cross-sections normal to the trench are shown in Figure 5. Figure 5a shows the section nearest to the Tehuantepec ridge, where location errors are large due to the lack of a seismic station in the Isthmus of Tehuantepec. This profile suggests a dip of  $35^\circ$  of the W-B zone. Profiles 5b, 5c and 5d suggest an increasing to  $40^\circ \pm 2^\circ$ . In conclusion, the angle of subduction increases from  $25^\circ$  at Oaxaca to  $30^\circ$  to  $35^\circ$  at the Isthmus of Tehuantepec in agreement with Pardo and Suárez, (1995) and  $40^\circ$  under Chiapas. The apparent hypocenter thickness of the subducted lithosphere (as defined by Schneider and Sacks, 1987) is 76 km in the Isthmus of Tehuantepec and  $39 \pm 4$  km in Chiapas.

### FOCAL MECHANISMS AND STRESS AXIS DISTRIBUTION

We used first motions to determine focal mechanisms of individual earthquakes, and composite focal mechanisms of clustered events within the subducting lithosphere. Sixteen single and composite focal mechanisms were obtained. Composite focal mechanisms were obtained for selected events within a radius of 10 km of one another in non-overlapping regions. Table 3 shows the focal parameters obtained. Composite focal mechanisms are identified as “C” and focal mechanisms reported by PDE since 1989 with magnitudes greater than 6 are shown as “P”. Plots of first-motion polarities in the lower-hemisphere projection are shown in Figure 6. Figure 7 shows the distribution of focal mechanisms in the area of study. Figure 8 shows a profile of seismicity and a side view of focal mechanisms along section C-C’.

Note that mechanism 7C indicates compression at the trench while mechanisms 6C, 8C and 10C indicate tension along the interplate boundary. Deeper events, between 50 and 200 km, show a mixed pattern of stresses. Event 19P at a depth of 164 km is a 7.2 magnitude event that occurred on October 21, 1995. Our polarity reading agrees with the Harvard solution and suggests that the subducted slab be under tension at this depth. Inversion of broadband body waves indicates that the rupture of this earthquake propagated up-dip from northwest to southeast along the strike of the subducted slab (Rebollar et al., 1998). Events with depths greater than 200 km clearly indicate down-dip compression inside the subducted slab.

We grouped the events by focal mechanism into two groups: events with hypocenters between 100 to 200 km and events deeper than 200 km. Figure 9(a) shows P and T axes

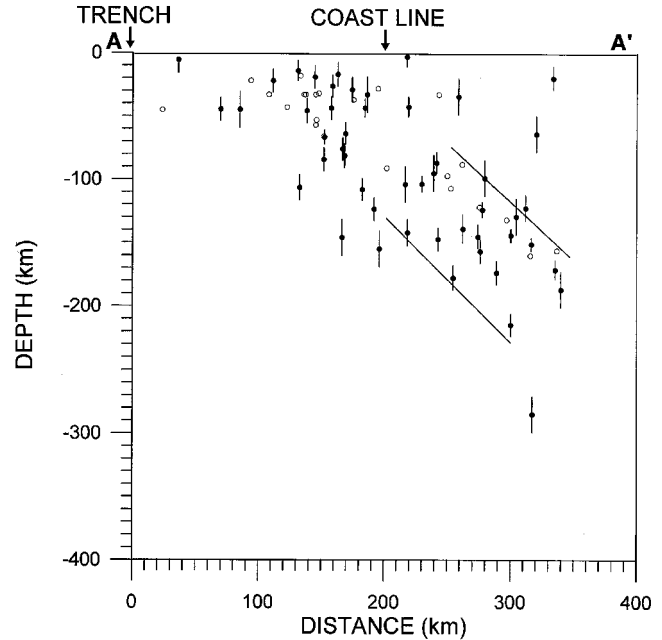


Fig. 5a. Cross section of the seismicity along profile A-A'. Vertical lines are location errors. This cross section is close to the Isthmus of Tehuantepec. The continuous line is our inference of the dip of the Wadati-Benioff zone fitted by eye. Apparent thickness of slab is of the order of 76 kilometers, and could have a large error since seismic stations are outside of this cross section. Open dots are events reported by PDE with magnitudes greater than 5 from 1978 to 1995. Events reported by Burbach et al. (1984) are included.

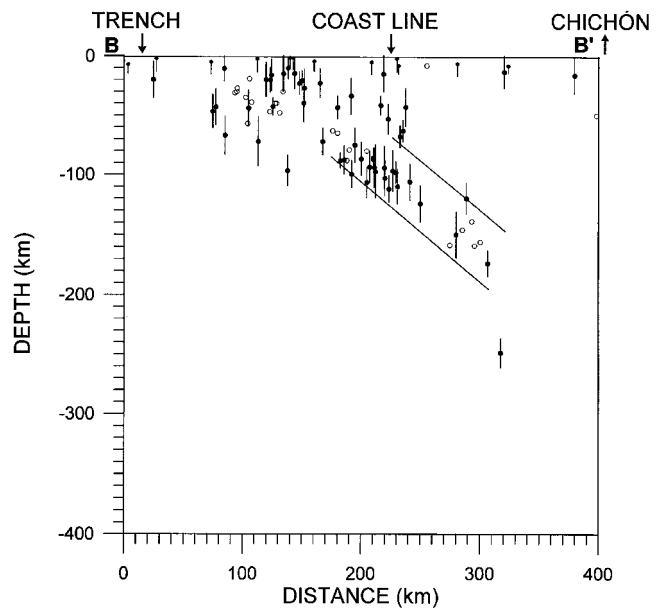


Fig. 5b. Cross section of seismicity along profile B-B'. Vertical lines are location errors. Continuous lines show our inference of the dip of the Wadati-Benioff zone. Open dots are events reported by PDE with magnitudes greater than 5 from 1978 to 1995. Events reported by Burbach et al. (1984) are included.

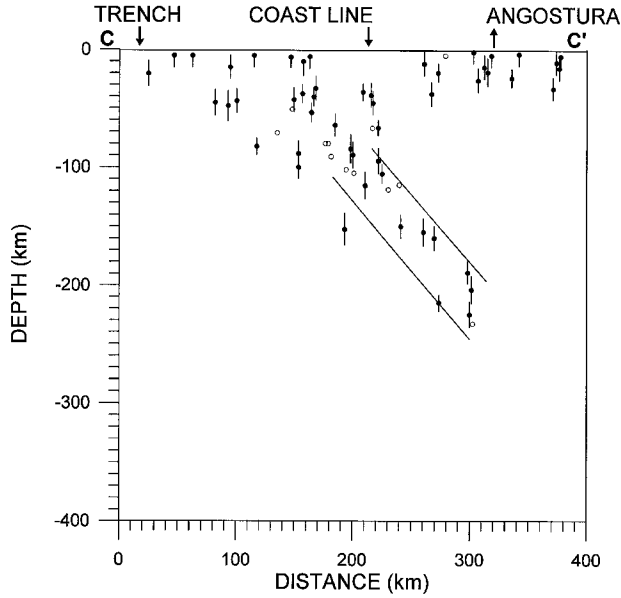


Fig. 5c. Cross section of seismicity along profile C-C'. Continuous lines show our inference of the dip of the Wadati-Benioff zone as well as the apparent range of hypocenters. Open dots are events reported by PDE with magnitudes greater than 5 from 1978 to 1995. Events reported by Burbach *et al.* (1984) are included.

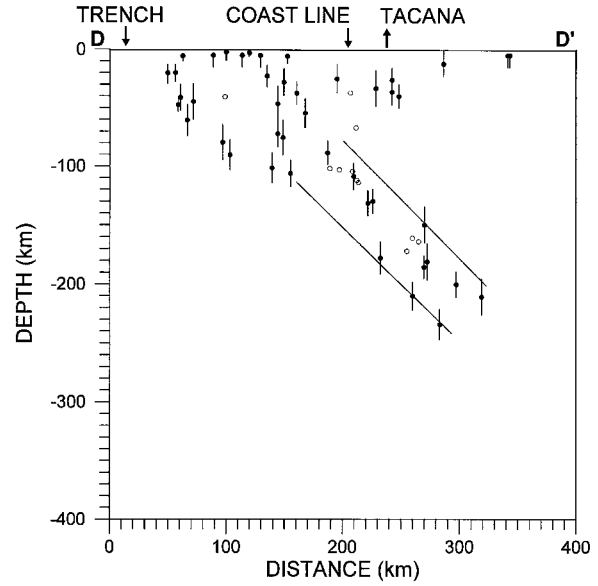


Fig. 5d. Cross section of seismicity along profile D-D'. Continuous lines show our inference of the dip of the Wadati-Benioff zone as well as the apparent range of hypocenters. Open dots are events reported by PDE with magnitudes greater than 5 from 1978 to 1995. Events reported by Burbach *et al.* (1984) are included.

Table 3

Focal mechanism parameters ( $\Phi$  = Strike,  $\delta$  = dip,  $\lambda$  = rake)

| LOCATION |         |              | FAULT PLANE A |            |             | T     |        | P     |        | ID  |
|----------|---------|--------------|---------------|------------|-------------|-------|--------|-------|--------|-----|
| LAT.     | Lon.    | DEPTH.<br>km | $\Phi$ °      | $\delta$ ° | $\lambda$ ° | TREND | PLUNGE | TREND | PLUNGE |     |
| 16.239N  | 92.996W | 189          | 325           | 80         | 90          | 235   | 55     | 55    | 35     | 1   |
| 16.528N  | 93.135W | 248          | 146           | 85         | -90         | 236   | 40     | 56    | 50     | 2   |
| 15.111N  | 93.179W | 64           | 122           | 13         | 90          | 212   | 58     | 32    | 32     | 3   |
| 15.782N  | 92.619W | 213          | 334           | 85         | 90          | 244   | 50     | 64    | 40     | 4   |
| 15.232N  | 91.528W | 272          | 309           | 85         | 90          | 219   | 50     | 39    | 40     | 5   |
| 15.165N  | 93.883W | 15           | 125           | 46         | -90         | 215   | 1      | 35    | 89     | 6C  |
| 13.833N  | 93.280W | 10           | 316           | 45         | 90          | 90    | 90     | 46    | 00     | 7C  |
| 14.083N  | 92.000W | 35           | 300           | 52         | -111        | 45    | 4      | 150   | 72     | 8C  |
| 16.450N  | 92.776W | 20           | 90            | 57         | 119         | 51    | 64     | 160   | 8      | 9   |
| 15.858N  | 94.581W | 15           | 109           | 66         | -131        | 228   | 12     | 333   | 50     | 10C |
| 15.416N  | 93.466W | 85           | 307           | 59         | 90          | 217   | 76     | 37    | 14     | 11C |
| 16.591N  | 94.706W | 159          | 356           | 52         | -122        | 108   | 2      | 203   | 65     | 12C |
| 15.666N  | 93.833W | 100          | 313           | 47         | 90          | 223   | 88     | 43    | 2      | 13C |
| 15.701N  | 92.827W | 153          | 325           | 45         | -90         | 55    | 00     | 90    | 90     | 14C |
| 17.485N  | 94.998W | 120          | 289           | 70         | -120        | 41    | 19     | 160   | 54     | 15C |
| 15.260N  | 92.723W | 135          | 117           | 84         | 90          | 27    | 51     | 207   | 39     | 16C |
| 16.05N   | 93.70W  | 112          | 354           | 89         | -45         | 50    | 29     | 300   | 31     | 17P |
| 15.98N   | 92.64W  | 168          | 138           | 84         | 119         | 76    | 43     | 204   | 32     | 18P |
| 16.67N   | 93.42W  | 164          | 313           | 90         | -103        | 56    | 43     | 210   | 43     | 19P |
| 15.83N   | 93.18W  | 82           | 311           | 68         | -92         | 43    | 23     | 218   | 66     | 20P |

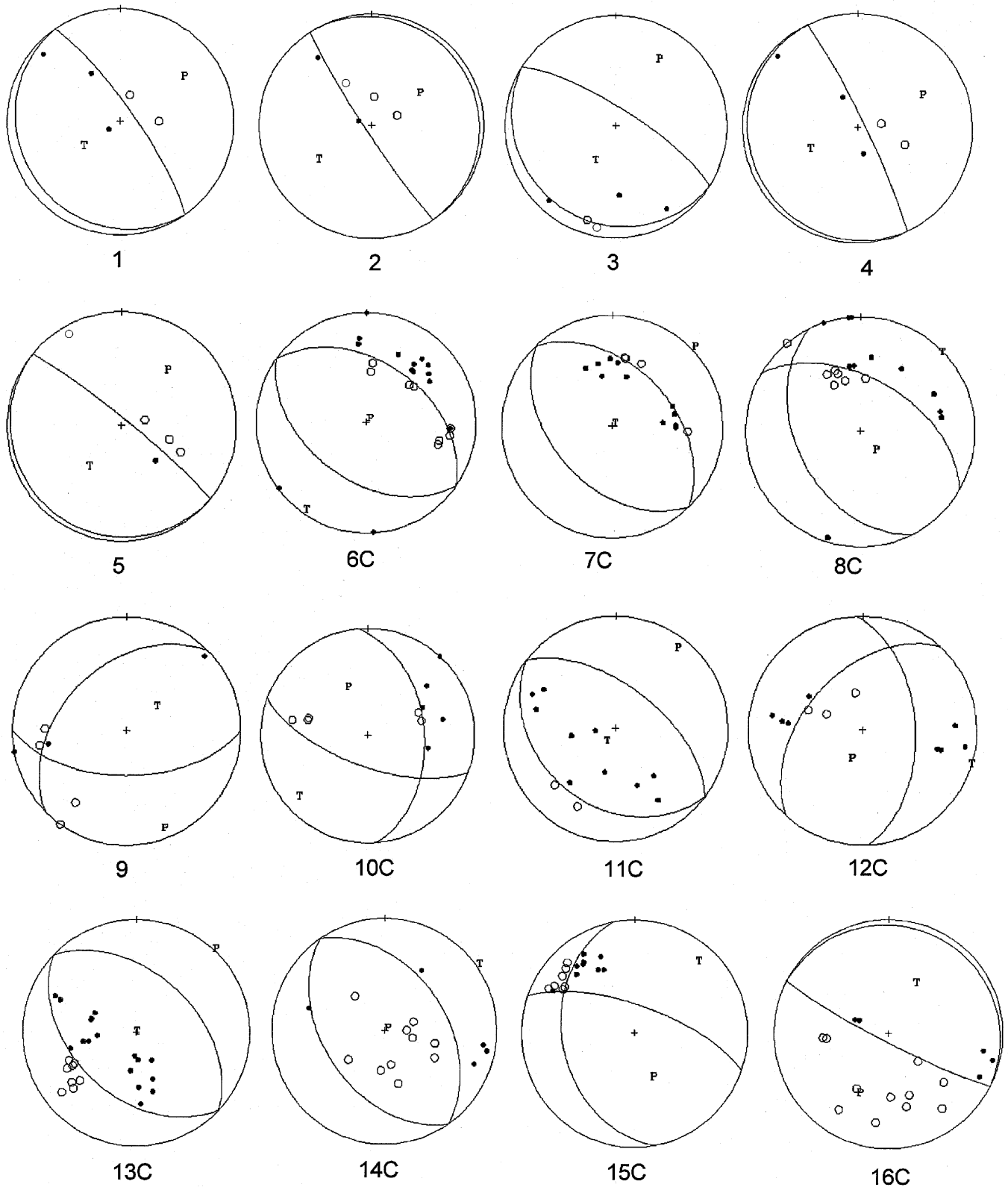


Fig. 6. P-wave motion data of all the events on a lower hemisphere projection. Dots denote compressional and empty dots denote dilatational first motions. P (full circles) and T (open circles) denote compressional and tensional axes. Parameters are listed in Table 4.

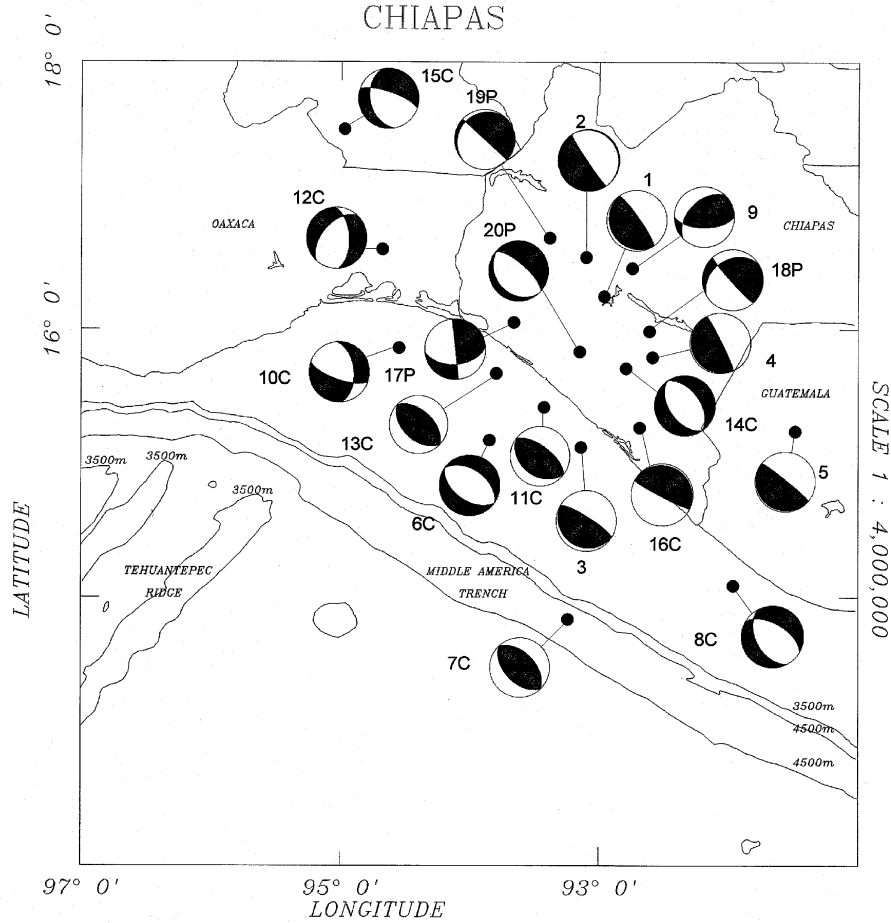


Fig. 7. Focal mechanisms on lower hemisphere projection. Compressional quadrants are solid. C indicates composite focal mechanisms and P focal mechanisms reported by Harvard since 1989, for magnitudes greater than 6. The event numbers refer to Table 3.

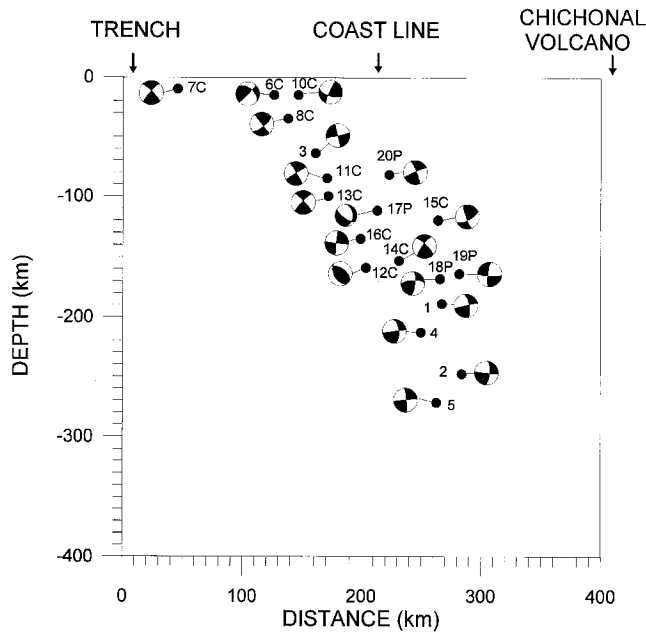


Fig. 8. Cross section along profile C-C'. Focal mechanisms are represented in a side view.

on an equal-area between 100 and 200 km. T and P axes are not consistent in this range of depths; however, T and P are aligned with the subducted plate and the convergence direction. Only three events with depths greater than 200 km are shown (Figure 9b). The plot of P and T shows that the deepest part of the subducted lithosphere is in down-dip compression.

Molnar and Sykes (1969), Dean and Drake (1978), Yamamoto and Mitchell (1988), Astiz *et al.* (1988), and Guzmán-Speziale *et al.* (1989) discussed focal mechanisms of Chiapas. Our events were located between longitude 91° and 95° west. One group of events had depths less than 50 km and a second group had depths between 50 and 100 km. Astiz *et al.* (1988) reported two events with depths greater than 100 km and Burbach *et al.* (1984) reported an event at a depth of 158 km, none of which are considered in this analysis. The P and T axes of all other published focal mechanisms are shown in Figure 10. The arrows indicate the direction of convergence of the Cocos plate in Chiapas (DeMets *et al.*, 1990). Figure 10-a shows events with a depth of up to 50 km; here 70% of the tension axes dip is found between

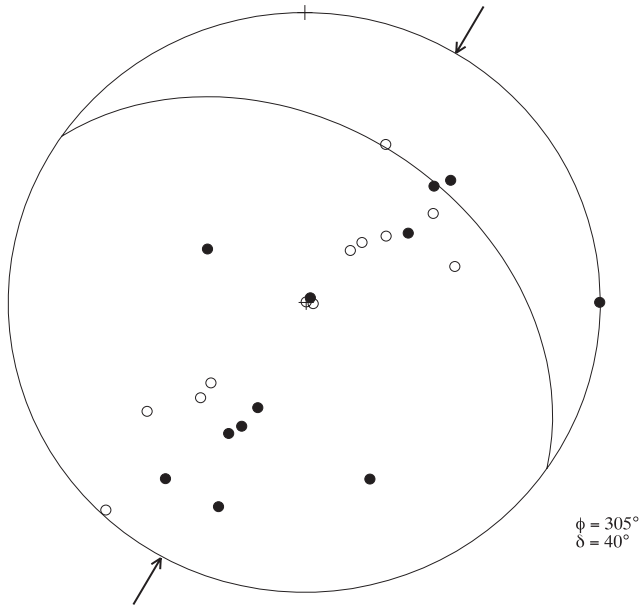


Fig. 9a. Plot of P and T axes on an equal area lower projection of events with depths between 100 and 200 km. Tension (open circles) and compression (solid circles) axes are aligned with the subducted plate and convergence direction. A mixed pattern of down-dip tension and compression is observed in this depth range. Arrows indicate the direction of convergence of the Cocos plate.  $\phi=305^\circ$  and  $\delta=40^\circ$  are the strike and dip of the Cocos plate.

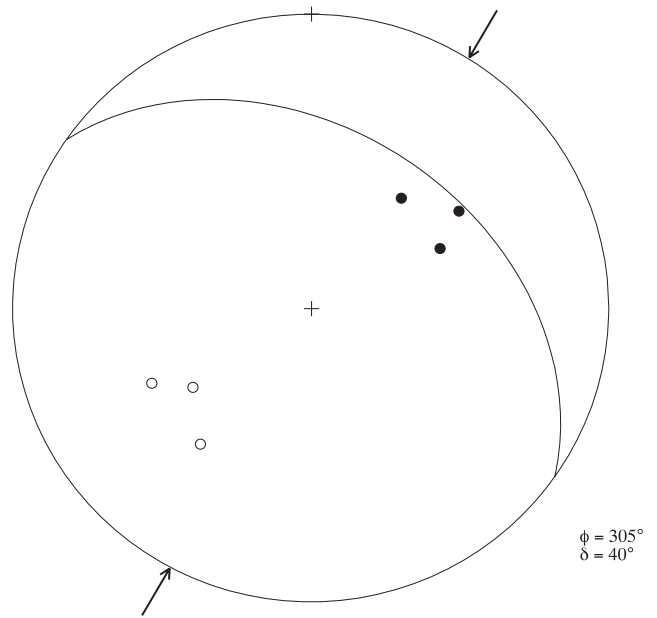


Fig. 9b. Plot of P (solid circles) and T (open circles) axes on an equal area lower projection of events with depths between 200 and 300 km. P and T axes show that the bottom part of the subducted lithosphere is in down-dip compression. Arrows indicate the direction of convergence of the Cocos plate.  $\phi=305^\circ$  and  $\delta=40^\circ$  are the strike and dip of the Cocos plate.

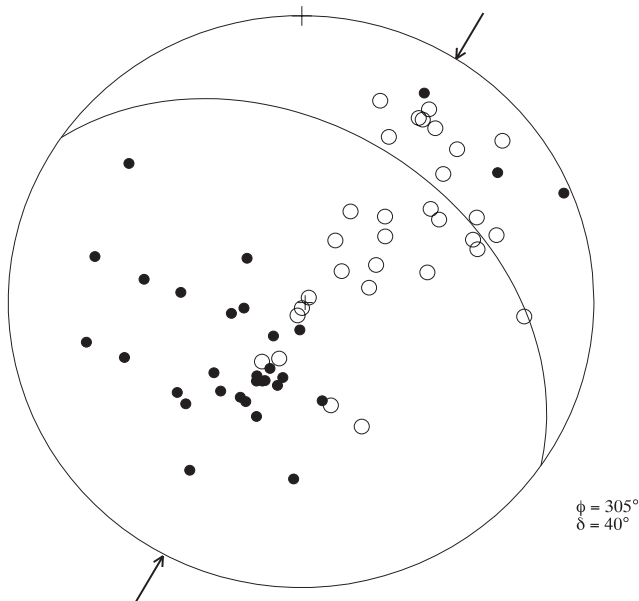


Fig. 10a. Plot of P (solid circles) and T (open circles) axes of published focal mechanisms of events up to a depth of 50 km. The data was taken from Molnar and Sykes (1969), Dean and Drake (1978), Yamamoto and Mitchell (1988), Astiz *et al.* (1988) and Guzmán-Speziale *et al.* (1989). At this depth range the subducted lithosphere is mainly in down-dip tension at dips between  $15^\circ$  to  $45^\circ$  (see text). Arrows indicate the direction of convergence of the Cocos plate.  $\phi=305^\circ$  and  $\delta=40^\circ$  are the strike and dip of the Cocos plate.

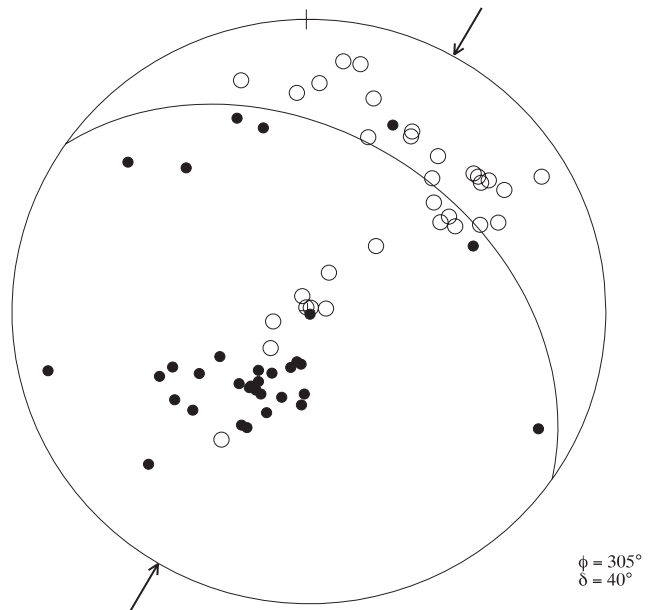


Fig. 10b. Plot of P (solid circles) and T (open circles) axes of published focal mechanisms of events between 50 and 100 km. The data was taken from Molnar and Sykes (1969), Dean and Drake (1978), Yamamoto and Mitchell (1988), Astiz *et al.* (1988) and Guzmán-Speziale *et al.* (1989). Again, the subducted lithosphere is in down-dip tension; however, there is a broad range in dip-directions of T axes. Arrows indicate the direction of convergence of the Cocos plate.  $\phi=305^\circ$  and  $\delta=40^\circ$  are the strike and dip of the Cocos plate.

15° and 45° in the convergence direction, indicating that the subducted crust is under tension. Compression axes cluster mainly around 220° azimuth, and 60° dip. At depths between 50 and 100 km (Figure 10b), 72% of the tension axes scatter between 20° to 75° dip suggesting a complex pattern of stress distribution in this depth range.

### CONCLUSIONS

Details of the subducted Cocos plate along the down-dip have been estimated from the seismicity recorded in a portable network deployed at Chiapas. S-wave velocities were estimated using a Poisson's ratio of 0.24 calculated from a Wadati diagram. Our data suggests a smooth increase in the dip angle from 25° at Oaxaca, 35° at the Isthmus of Tehuantepec and 40° below Chiapas. Apparent hypocenter thickness of the subducted slab under Chiapas is of the order of 39±4. Previous focal mechanism solutions in this sector of the Middle America Trench have been calculated for events not deeper than 100 kilometers. Those studies have shown that tension (T) axes spread in a range of dips from 20° to 75° along the convergence of the Cocos plate, which indicates that stresses along the bending of the subducted plate are mainly tensional stresses. We plotted vertical profiles of seismicity and focal mechanisms. We found that shallow events near the trench of the downgoing lithosphere are mainly tensional stresses, in agreement with the focal mechanism already published. At intermediate depths, between 100 and 200 kilometers, there is a mixed pattern of tension and pressure axes along the down-dip of the subducted slab. At depths greater than 200 kilometers the subducted lithosphere is under compression.

### ACKNOWLEDGMENTS

The authors are grateful to Luciana Astiz, Geoffrey Abers and Cinna Lomnitz for their helpful suggestions for improving this manuscript. We would like to thank the National Council of Science and Technology of Mexico (CONACYT) for sponsoring part of this project (Projects 3389-T9309 and 4292P-T). One of us (V. H. E.) was supported by a scholarship from CONACYT.

### BIBLIOGRAPHY

- ASTIZ, L., T. LAY and H. KANAMORI, 1988. Large intermediate-depth earthquakes and the subduction process. *Phys. Earth and Planet. Int.*, 53, 80-166.
- BURBACH, G. V., C. FROHLICH, W. D. PENNINGTON and T. MATUMOTO, 1984. Seismicity and Tectonics of the Subducted Cocos Plate. *J. Geophys. Res.*, 89, 7719-7735.
- BEVIS, M. and B. L. ISACKS, 1984. Hypocentral trend surface analysis: Probing the geometry of Benioff Zones. *J. Geophys. Res.*, 89, 6153-6170.
- CASTRO, R., 1980. Un modelo de la corteza terrestre para el sur de México mediante el uso de sismos profundos, Tesis profesional, Facultad de Ingeniería, UNAM, México.
- COUCH, R. and S. WOODCOCK, 1981. Gravity and structure of the continental margins of southwestern Mexico and northwestern Guatemala. *J. Geophys. Res.*, 86, 1829-1840.
- DEAN, B. W. and C. L. DRAKE, 1978. Focal mechanism solutions and tectonics of the Middle America arc. *J. Geol.*, 86, 111-128.
- DEMETS, C., R. G. GORDON, D. F. ARGUS and S. STEIN, 1990. Current plate motions. *Geophys. J. Int.*, 101, 425-478.
- GUZMAN-SPEZIALE, M., W. D. PENNINGTON and T. MATUMOTO, 1989. The triple junction of the North America, Cocos, and Caribbean plates. *Seism. Tect.*, 8, 981-997.
- HANUS, V. and J. VANEK, 1978. Subduction of the Cocos plate and deep active fracture zones of Mexico. *Geofis. Int.*, 17, 14-53.
- HAVSKOV, J., S. K. SINGH and D. NOVELO, 1982. Geometry of the Benioff in the Tehuantepec area in southern Mexico. *Geofis. Int.*, 21, 325-330.
- LAY, T. and T. C. WALLACE, 1995. Modern Global Seismology, Academic Press.
- LEE, W. H. K. and J. C. LAHR, 1972. HYPO71: A computer program for determining hypocenter, magnitude, and first motion pattern of local earthquakes. U. S. Geol. Survey, Open-File report.
- LEFEVRE, L. V. and K.C. McNALLY, 1985. Stress distribution and subduction of aseismic ridges in the Middle America subduction zone. *J. Geophys. Res.*, 90, 4495-4510.
- LIGORRIA, J. P. and E. MOLINA, 1997. Crustal structure of southern Guatemala using refracted and Sp converted waves. *Geofis. Int.*, 36, 9-19.
- LIGORRIA, J. P. and L. PONCE, 1993. Estructura cortical en el Istmo de Tehuantepec, México, usando ondas convertidas. *Geofis. Int.*, 32, 89-98.
- MATUMOTO, T., M. OHTAKE, G. LATHAN and J. UMANA, 1977. Crustal structure in southern Central America. *Bull. Seism. Soc. Am.*, 77, 2,095-2,114.

- McCANN, W., S. NISHENKO, L. SYKES and J. KRAUSE, 1979. Seismic gap and tectonics: seismic potential for major boundaries. *Pageoph*, 117, 1,082-1,147.
- McNALLY, K. C. and B. MINSTER, 1981. Nonuniform seismic slip rates along the Middle America Trench. *J. Geophys. Res.*, 86, 4,949-4,959.
- MOLNAR, P. and L. R. SYKES, 1969. Tectonics of the Caribbean and Middle-America regions from focal mechanisms and seismicity. *Geol. Soc. Am. Bull.*, 80, 1,639-1,684.
- PONCE, L., R. GAULON, G. SUAREZ and E. LOMAS, 1992. Geometry and state of stress of the downgoing Cocos plate in the Isthmus of Tehuantepec, Mexico. *Geophys. Res. Lett.*, 19, 773-776.
- PACHECO, J. F. and L. R. SYKES, 1992. Seismic moment catalog of large shallow earthquakes, 1900 to 1989. *Bull. Seism. Soc. Am.*, 82, 1306-1349.
- PACHECO, F. J., L. R. SYKES and C. H. SCHOLZ, 1993. Nature of seismic coupling along simple plate boundaries of subduction type. *J. Geophys. Res.*, 98, 14113-14159.
- PARDO, M. and G. SUAREZ, 1995. Shape of the subducted Rivera and Cocos plates in southern Mexico: Seismic and tectonic implications. *J. Geophys. Res.*, 100, 12,357-12,373.
- REBOLLAR, C. J., L. QUINTANAR, J. YAMAMOTO and A. URIBE, 1998. Source process of the Chiapas, Mexico, intermediate depth earthquake ( $M_w=7.2$ ) October 21, 1995. Submitted to the Bulletin of the Sismological Society of America.
- RUFF, L. F. and A. D. MILLER, 1994. Rupture process of large earthquakes in the northern México subduction zone. *Pageoph*, 142, 101-171.
- SINGH, S. K. and M. MORTERA, 1991. Source time functions of large Mexican subduction earthquakes, morphology of the Benioff zone, age of the plate, and their tectonic implications. *J. Geophys. Res.*, 96, 21,487-21,502.
- SINGH, S. K., L. ASTIZ and J. HAVSKOV, 1981. Seismic gaps and recurrence periods of large earthquakes along the Mexican subduction zone: a reexamination. *Bull. Seism. Soc. Am.*, 71, 827-843.
- SCHNEIDER, J. F. and I. S. SACKS, 1987. Stress in the contorted Nazca plate beneath southern Peru from local earthquakes. *J. Geophys. Res.*, 92, 13887-13902.
- SUAREZ, G., J. P. LIGORRIA and L. PONCE, 1992. Preliminary crustal structure of the coast of Guerrero, Mexico, using the minimum apparent velocity of refracted waves. *Geofis. Int.*, 31, 247-252.
- THATCHER, W., 1990. Order and diversity in the modes of circum-Pacific earthquakes recurrence. *J. Geophys. Res.*, 95, 2609-2623.
- YAMAMOTO, J. and B. J. MITCHELL, 1988. Rupture mechanics of complex earthquakes in southern Mexico. *Tectonophys.*, 154, 25-40.

---

Cecilio J. Rebollar<sup>1</sup>, Victor H. Espíndola<sup>1</sup>, Antonio Uribe<sup>2</sup> Antonio Mendoza<sup>1</sup> and Arturo Pérez-Vertti<sup>1</sup>

<sup>1</sup> CICESE, Earth Science Division, Km 107 Carretera Tijuana-Ensenada, Baja California, México.  
E-mail rebollar@cicese.mx

<sup>2</sup> CFE, Gerencia de Estudios de Ingeniería Civil, Departamento de Sismotectónica. Oklahoma 85, Col. Nápoles 03810, México, D. F., México.